Optimizing the Code Rate of Energy-Constrained Wireless Communications with HARQ

Fernando Rosas*, Richard Demo Souza†, Marcelo Pellenz‡, Christian Oberli§‖, Glauber Brante†, Marian Verhelst* and Sofie Pollin*

*KU Leuven, Belgium

†Federal University of Technology – Paraná, Brazil

‡Pontifical Catholic University of Paraná, Brazil

§Pontificia Universidad Católica de Chile, Chile

‖National Research Center for Integrated Natural Disaster Management, Chile.

Abstract

Retransmissions due to decoding errors have a big impact on the energy budget of low-power wireless communication devices, which can be reduced by using hybrid automatic repeat request (HARQ) techniques. Nevertheless, this reduction comes at the cost of extra energy consumption introduced by the added computational load. No complete analysis of the trade-off between retransmissions reduction and baseband consumption of low-power communications over fading channels has been reported so far.

In this article, we study the energy efficiency achievable by HARQ schemes when the code rate of the error-correcting code is optimized. The analysis focuses on the case of simple HARQ (S-HARQ) and Chase combining (HARQ-CC), which are studied under fast-fading and block-fading scenarios with Nakagami-m fading. The retransmission statistics are analyzed and expressions for the expected number of transmission trials are derived. Using this framework, it is shown that transmission schemes with high diversity gain are the most efficient choice for long range transmissions, which in our case corresponds to HARQ-CC and codes with low code rate. On the other hand, schemes with good multiplexing capabilities are optimal for short link distances, which in our analysis corresponds to S-HARQ and high code rates. It is also shown that HARQ-CC can effectively extend the transmission range of a low-power communication device.

I. Introduction

The development of techniques for reducing the energy consumption of wireless communications is a central requirement for technologies like wireless sensor networks (WSN) to prosper into large-scale autonomous systems. The main tasks that the nodes of these networks perform are sensing the environment, processing the data and communicating it wirelessly across the network. The latter task dominates the overall energy budget and, therefore, optimizing it has a direct impact on the network lifetime [1]. In fact, battery depletion has been identified as one of the primary causes of lifetime limitation of these networks [2]. Replacing batteries regularly is impractical in large networks or even impossible in hostile or remote environments [3].

The communication energy budget depends on choices such as the transmission power and data framing structure, which have a direct impact on the frame error rate (FER) [1]. The FER, in turn, determines the average number of necessary retransmissions and therefore also affects the overall energy needed to convey successfully each bit of information from one node to the next. In fact, it has been shown that retransmissions can be a dominant factor in the energy budget of low-power communications [4], [5].

Automatic repeat request (ARQ) is an interesting tool for reducing the impact of retransmissions on the overall energy budget of low-power devices. In effect, the recent literature reports an increasing interest on the energy efficiency of hybrid-ARQ (HARQ) schemes, which handle the retransmissions using various channel coding techniques. Collaborative and non-collaborative HARQ systems under an outage constraint are studied in [6], where it is shown that the optimal irradiated energy depends both on the number of retransmissions and on the consumption of the electronic components of the transceivers. In [7], simple HARQ, HARQ with Chase combining (CC) and HARQ with incremental redundancy (IR) are considered when either an outage constraint is imposed or the transmission rate is optimized in order to maximize the throughput. HARQ in space-time coding (STC)-based systems has been studied in terms of energy-limited outage probability in [8]. Results show that the energy efficiency is substantially improved by the combination of retransmissions and STC techniques when the transmitted power allocation is optimized.

The energy consumption models considered in the cited references are based on the notion of channel capacity, which plays a key role in linking the rate of information transfer, the signal-to-noise ratio (SNR) and the energy consumption. This link has been established

in two alternative ways: one approach is to define energy efficiency as the ratio between the link capacity and the average power required by the communication process [9], [10], while the second alternative is to consider the system outage probability [6]–[8]. However, using the channel capacity forces to assume that capacity-achieving error correcting codes (ECC) are employed, whose significant processing costs should not be left out of the energy consumption budget —as is usually done in the literature. In fact, while high-performance codes provide better error correcting performance, they require more elaborated and hence less energy-efficient decoders than simpler codes. An analysis which follows this line of thought can be found in [11], where the authors examine the energy efficiency of specific ECC implementations in WSNs. The approach focuses on complex iterative codes, such as turbo or low-density parity-check codes (LDPC) which are not well suited to the computational capabilities of WSN nodes, and only considers transmissions over additive white Gaussian noise channels (AWGN).

The combined energy efficiency of simple HARQ and ECC over fading channels has been investigated in [12] and [13] by analyzing a Bluetooth network, and in [14] where a general approach for sensor networks is provided. Nevertheless, these works do not take into account the power consumption of electronic circuits and the results are restricted to convolutional codes. The combination of simple HARQ with convolutional codes is also considered in [15], where the authors aim at the best configuration of the wireless link protocol in order to guarantee a given performance at the transport layer with the TCP protocol. Nevertheless, [16] showed that BCH codes can be up to 15% more energy-efficient than the best performing convolutional code. However, the analysis presented in [16] focuses on the optimization of the frame length for a fixed code rate and does not include the power consumption of electronic circuits in the analysis. Finally, [17], [18] present an interesting analysis of the energy efficiency of simple HARQ transmissions when using convolutional codes with rates 1/2 and 2/3, and turbo codes with rate 1/3 over Rayleigh channels. Unfortunately, it is not clear how to extend that framework in order to study more complex HARQ transmissions.

In this paper, we study the energy efficiency of simple HARQ (S-HARQ) and Chase combining (HARQ-CC) when the code rate is also a variable that can be optimized. Our analysis includes the energy cost of the baseband operations required for encoding and decoding, which is a relevant factor that has been over-simplified in most of the literature. Our analysis is focused on BCH and convolutional codes with a wide range of code rates, motivated by their flexibility while keeping the low-complexity requirements of WSNs. Also,

we have chosen to analyze HARQ-CC over other types of retransmission schemes like HARQ-IR, as the former gives more flexibility in terms of code choice.

In contrast to much of the available literature, our approach is not information theoretical but based on signal models. Following [4], [19], our work provides a novel approach for accounting for the costs of retransmissions due to decoding errors of concrete modulation and channel coding schemes over various channel fading models. In particular, we provide formulas for the retransmission statistics of S-HARQ and HARQ-CC in fast-fading and block-fading Nakagami-m channels, which represent the efficiency of the retransmission scheme. Note that our approach avoids using the channel capacity, but calculates directly the energy consumption per data bit transferred without error considering the required number of retransmissions. The results obtained with our model allow for practical interpretations, providing guidance for the joint optimization of the irradiated power, modulation size and code rate of concrete HARQ schemes. Moreover, we introduce the notion of *energy-optimal code rate*, which represents the amount of redundancy required for achieving the highest energy-efficiency in a given communication system. We show that the optimal code rate is low for long transmission distances and high for short range communications.

The rest of this article is structured as follows. First, Section II develops a general model of the energy consumption required for attaining error-free data transmission over a wireless link. It is a general model, in the sense that it allows for analyzing systems with any type of channel coding scheme and any kind of retransmission regulation policy. We illustrate the use of the model for the particular cases of BCH and convolutional codes, for which we precisely quantify the energy consumption of the encoding and decoding operations. Then, Section III considers S-HARQ and HARQ-CC transmissions, analyzing their retransmission statistics under Nakagami-m channels. Then, using these results, Section IV presents an optimality analysis with regard to several transmission parameters captured by our energy consumption model. The finding of this section are then confirmed by numerical evaluations, presented in Section V. Finally, Section VI summarizes our conclusions.

II. Energy consumption model

The goal of this section is to determine the total energy that is necessary for transferring one bit of data successfully, henceforth called a *goodbit*, in a point-to-point packet-switched wireless communication. Following [4], it is assumed that every frame transmitted in the *forward* direction is matched by a feedback frame in the *reverse* direction that acknowledges

correct reception or requests a retransmission. It is also assumed that the irradiated power is determined based upon knowledge of the statistics of the SNR at the decision stage of the receiver. It is further assumed that all frames in both directions are always detected and that all feedback frames are decoded without error.

In the sequel, Section II-A analyses the energy consumption from the standpoint of a transceiver that transmits one forward payload frame and receives the corresponding feedback frame (the reverse case —a transceiver that receives one payload frame and transmits the corresponding feedback frame— follows by analogy). Section II-B then synthesizes the total energy consumption model.

A. Components of Energy Consumption of the Forward Transceiver

The energy consumption of the transceiver that transmits forward frames and receives feedback frames is composed of six terms, each one described next.

1) Consumption of Electronic Components of the Transceiver due to Pre-transmission Processing: Let us define $r = k/n$ as the code rate, where n is the number of bits per codeword and $n-k$ is the number of redundant bits. Then, each physical-layer forward frame carries L_{H} bits of header with essential transmission parameters and a payload composed by rL_{P} bits of data and $(1-r)L_{\mathrm{P}}$ additional bits for coding.

The total duration of a forward frame is shared by T_{O} seconds for the transmission of overhead signals for acquisition and tracking (channel estimation, synchronization, etc.), T_{H} seconds for the transmission of the header (with a binary modulation) and T_{P} seconds for transmitting the L_{P} bits of payload (with a suitable modulation). The average air time per data bit in a forward frame is hence $T_{\mathrm{b}} = (T_{\mathrm{O}}+T_{\mathrm{H}}+T_{\mathrm{L}})/(rL_{\mathrm{P}})$. Let us assume that the payload is encoded using an M-ary modulation, so that each payload symbol therefore carries $\log_2(M)$ bits. If R_{s} denotes the physical layer symbol-rate, then T_{b} can be formulated as

$$T_{\mathrm{b}} = \frac{1}{rR_{\mathrm{s}}}\left(\frac{1}{\log_2(M)} + \frac{L_{\mathrm{H}}+L_{\mathrm{O}}}{L_{\mathrm{P}}}\right) \ , \tag{1}$$

where L_{O} is a measure, in bits, of the total overhead per forward frame.

Following (1), one may write the energy per bit per forward frame used for transmit processing as

$$\mathcal{E}_{\text{el,tx}} = P_{\text{el,tx}} T_{\mathrm{b}} \ , \tag{2}$$

where $P_{\text{el,tx}}$ is the power consumption of the baseband and radio-frequency electronic components that perform the forward transmission. It is to be noted that $\mathcal{E}_{\text{el,tx}}$ is largely dominated

by passband processing components such as filters, mixers and frequency synthesizers [20].

2) Energy Consumption due to Electromagnetic Irradiation: Each frame is emitted with a transmission power P_{tx} provided by the power amplifier (PA). The PA's power consumption is modeled by

$$P_{\text{tx}} = \frac{\eta}{\xi} P_{\text{PA}} \ , \tag{3}$$

where ξ is the peak-to-average ratio of the transmitted signal and η is the drain efficiency of the PA [21]. Thus, the energy per bit per forward frame due to electromagnetic irradiation is

$$\mathcal{E}_{\text{PA}} = P_{\text{PA}} T_{\text{b}} \ , \tag{4}$$

where T_{b} is given by (1).

Let us express P_{PA} as a function of the mean SNR $\bar{\gamma}$. The transmission power attenuates over the air with path loss and arrives at the receiver with a mean power given by

$$P_{\text{rx}} = \frac{P_{\text{tx}}}{A_0 d^{\alpha}} \ , \tag{5}$$

where A_0 is a parameter that depends on the transmitter and receiver antenna gains and the transmission wavelength, d is the distance between transmitter and receiver and α is the path loss exponent [22]. At the input of the decision stage of the receiver, $\bar{\gamma}$ is related to P_{rx} as

$$\bar{\gamma} = \frac{P_{\text{rx}}}{N_0 W N_{\text{f}} M_{\text{l}}} \ , \tag{6}$$

where N_0 is the power spectral density of the baseband-equivalent additive white Gaussian noise, W is the bandwidth, N_{f} is the noise figure of the receiver's front end and M_{l} is a link margin term that represents any other unaccounted loss [21]. From (3), (5) and (6) it is found that

$$P_{\text{PA}}(\bar{\gamma}) = \left(\frac{\xi A_0 N_0 W N_{\text{f}} M_{\text{l}}}{\eta} \right) d^{\alpha} \bar{\gamma} = A d^{\alpha} \bar{\gamma} \ , \tag{7}$$

with A being a constant.

3) Energy Consumption of Electronic Components due to the Processing of Feedback Frames: For simplicity, feedback frames are assumed to be transmitted uncoded using a binary modulation. Hence, the transmission of each feedback frame lasts $L_{\text{F}}/R_{\text{s}}$ seconds, where L_{F} is the number of bits that compose the feedback frame and R_{s} is as defined in Section II-A1. During this time, the transceiver consumes $P_{\text{el,rx}}$ Watts, which mainly includes the power needed for energizing the passband receiver elements (low-noise amplifiers, mixers,

filters, frequency synthesizers, etc.) [20]. Therefore, the energy per forward bit spent by the transmitter for decoding the corresponding feedback frame is given by

$$\mathcal{E}_{\text{fb,rx}} = \frac{P_{\text{el,rx}} L_{\text{F}}}{r L_{\text{P}} R_{\text{s}}} = P_{\text{el,rx}} T_{\text{fb}} \ , \tag{8}$$

where $T_{\text{fb}} = L_{\text{F}}/(r R_{\text{s}} L_{\text{P}})$ is the feedback time per payload bit.

4) Baseband Electronic Consumption: Performing the encoding and decoding of each frame can be a demanding baseband operation*. Each encoding procedure involves J different kinds of arithmetic operations, each of which has an energy consumption $\mathcal{E}_j$ and is performed $n_j^{\text{enc}}(r)$ times during the encoding algorithm. Consider that the encoding has to be done once for each frame, and hence its cost is shared among the rL_{P} data bits. Therefore, the energy consumption for encoding one frame, ϵ_{enc}, is given by

$$\epsilon_{\text{enc}} = \sum_{j=1}^{J} \epsilon_j n_j^{\text{enc}}(r) \ . \tag{9}$$

If the operations are performed by an arithmetic processing unit (APU), the energy consumption of the j-th operation can be modeled as $\epsilon_j = V_{\text{dd}} I_0 \Delta t_j$, where V_{dd} is the APU operating voltage and I_0 is the average current during the execution time of the arithmetic operations [23]. It is to be noted that I_0 depends on V_{dd} and on the APU's clock frequency, f_{APU}. Δt_j is the time required for executing the j-th operation, which is related to f_{APU} and to the number of clock cycles required by the operation, c_j, as $\Delta t_j = c_j / f_{\text{APU}}$. By replacing these terms in (9) the energy required for encoding normalized per data bit, $\mathcal{E}_{\text{enc}}$, can be calculated as

$$\mathcal{E}_{\text{enc}} = \frac{\epsilon_{\text{enc}}}{r L_{\text{P}}} = \frac{V_{\text{dd}} I_0}{r L f_{\text{APU}}} \sum_{j=1}^{J} c_j n_j^{\text{enc}}(r) \ . \tag{10}$$

Note that it is straightforward to write an equation for the decoding cost equivalent to (10).

As an illustration of how (10) can be used, Table I provides the number of operations required for decoding BCH and convolutional codes with rate $r = k/n$ that can correct up to t_{c} errors per codeword of $n = L_{\text{P}}$ bits. Table I also contains the number of operations required for HARQ-CC transmissions in both fast- and block-fading scenarios, which will be needed in Section (II-B). The corresponding analysis can be found in Appendix A.

*Although other operations —e.g. the header and feedback processing— also consume energy, they are not included in the analysis as their consumption presents no significant variations among the considered transmission schemes.

TABLE I: Number of required operations per frame per transmission trial

Scheme	Additions	Products	Integer comp.	Binary comp.
BCH codes	$(2L_{\mathrm{P}}-1)t_{\mathrm{c}}+2t_{\mathrm{c}}^2$	$2L_{\mathrm{P}}t_{\mathrm{c}}+2t_{\mathrm{c}}^2$	–	–
Convolutional codes	$L_{\mathrm{P}}2^{k+\nu}$	–	$L_{\mathrm{P}}2^{\nu}(2^k-1)/n$	$L_{\mathrm{P}}2^{k+\nu}$
Punctured conv. codes	$L_{\mathrm{P}}2^{\nu+1}$	–	$rL_{\mathrm{P}}2^{\nu}$	$L_{\mathrm{P}}2^{\nu+1}$
HARQ-CC (fast-fading)	$2L_{\mathrm{P}}$	L_{P}	–	–
HARQ-CC (block-fading)	$L_{\mathrm{P}}+1$	L_{P}	–	–

5) Re-transmission Statistics: A key contributor to the energy consumption is the need for retransmissions due to forward frames that get decoded with errors at the receiver. The number of transmission trials needed until a frame is decoded without error, τ, is a random variable, whose distribution depends on physical layer parameters such as the SNR, channel statistics and modulation type, and on link layer parameters such as code rate, frame size and retransmission scheme.

Let us define z to be the maximum number of successive transmission trials for transmitting each forward frame before a *channel outage* event is declared. An outage declaration causes the system to enter a sleep period (i.e. a low-power mode) for at least one channel coherence time. After this, the system wakes up and attempts a new set of transmissions, which either ends with a correctly decoded frame or with a new series of z consecutive frame decoding errors. This process is repeated until the frame is decoded by the receiver without errors. Therefore, by defining τ_{out} as the number of outage declarations that occur before a frame is decoded without errors, one can express τ as

$$\tau = z\tau_{\text{out}} + \tau_z \ , \tag{11}$$

where τ_z is the trial index within the current set of transmission attempts. This variable is a discrete random variable that takes values in $\{0, 1, \ldots, z-1\}$, while both τ and τ_{out} can take any non-negative integer value. Their mean values are defined as $\bar{\tau}_z$, $\bar{\tau}$ and $\bar{\tau}_{\text{out}}$ respectively.

The statistics of τ and τ_{out} for S-HARQ and HARQ-CC are analyzed in Section III.

6) Startup Energy Consumption: The transmitter enters a low power consumption (sleep) mode each time an outage event is declared. Hence, it must be brought online before it can perform new transmissions. The time spent in the activation process, T_{st}, is largely dominated by the stabilization of the phase-lock-loop (PLL) [21]. For simplicity, in this work the startup

energy consumption is modeled as $\epsilon_{\text{st,tx}} = T_{\text{st}} P_{\text{el,tx}}$. Therefore, the startup energy per data bit per outage declaration can be calculated as $\mathcal{E}_{\text{st,tx}} = \epsilon_{\text{st,tx}}/(rL_{\text{P}})$, and the total startup energy consumption per goodbit is given by $\mathcal{E}_{\text{st,tx}}\tau_{\text{out}}$.

B. Total Energy per Successfully Transferred Bit

The material presented in Section II-A allows for stating our model of the total energy consumption. Concretely, the energy consumed per goodbit by the transmitter of forward frames, which also decodes feedback frames, is given by

$$\mathcal{E}_{\text{T}} = \mathcal{E}_{\text{st,tx}}\tau_{\text{out}} + \mathcal{E}_{\text{enc}} + (\mathcal{E}_{\text{el,tx}} + \mathcal{E}_{\text{PA}} + \mathcal{E}_{\text{fb,rx}})\,\tau \tag{12}$$

$$= \mathcal{E}_{\text{st,tx}}\tau_{\text{out}} + \mathcal{E}_{\text{enc}} + \left[(P_{\text{el,tx}} + P_{\text{PA}})\,T_{\text{b}} + P_{\text{el,rx}}T_{\text{fb}}\right]\tau \ . \tag{13}$$

By analogy, the total energy used by the receiver for demodulating τ forward transmissions and for transmitting the corresponding τ feedback frames is

$$\mathcal{E}_{\text{R}} = \mathcal{E}_{\text{st,rx}}\tau_{\text{out}} + \left[\mathcal{E}_{\text{dec}} + P_{\text{el,rx}}T_{\text{b}} + (P_{\text{el,tx}} + P_{\text{PA}})\,T_{\text{fb}}\right]\tau \ . \tag{14}$$

Above, $\mathcal{E}_{\text{st,rx}}$ is introduced as the startup consumption per data bit of the receiver, which is calculated as

$$\mathcal{E}_{\text{st,rx}} = \frac{T_{\text{st}}P_{\text{el,rx}}}{rL_{\text{P}}} \ . \tag{15}$$

Also, (14) introduces $\mathcal{E}_{\text{dec}}$ as the energy consumption of decoding the forward frame per data bit, which is given by

$$\mathcal{E}_{\text{dec}} = \frac{V_{\text{dd}}I_0}{rLf_{\text{APU}}} \sum_{j=1}^{J} c_j \left(n_j^{\text{dec}} + n_j^{\text{arq}}\right) \ , \tag{16}$$

where n_j^{dec} and n_j^{arq} indicate how many times the j-th operation is performed during the decoding algorithm and the retransmission method per transmission trial (c.f. Section II-A4).

The total energy consumption per goodbit, $\mathcal{E}_{\text{b}}$, is the sum of (13) and (14). Because of τ_{out} and τ, this quantity is a random variable that depends on the realizations of the channel and of the thermal noise. By using (7) and (20), it can be found that

$$\bar{\mathcal{E}}_{\text{b}} = \mathbb{E}\left\{\mathcal{E}_{\text{T}} + \mathcal{E}_{\text{R}}\right\} \tag{17}$$

$$= 2T_{\text{st}}P_{\text{el}}\bar{\tau}_{\text{out}} + \mathcal{E}_{\text{enc}} + [\mathcal{E}_{\text{dec}} + (P_{\text{el}} + Ad^{\alpha}\bar{\gamma})T]\bar{\tau} \ , \tag{18}$$

where $\mathbb{E}\{\cdot\}$ denotes the expectation operator, $P_{\text{el}} = P_{\text{el,tx}} + P_{\text{el,rx}}$ is the total power consumed by electronic components and $T = T_{\text{b}} + T_{\text{fb}}$ is the total time per data bit.

III. Retransmissions statistics

This section presents an analysis of the statistics of the retransmissions in various HARQ schemes. First, Section III-A studies S-HARQ statistics under fast-fading and block-fading channels, deriving exact expressions for the average number of transmission trials, $\bar{\tau}$, and the average number of outage declarations $\bar{\tau}_{\text{out}}$. It is also studied how these quantities depend on the maximum number of transmission attempts before declaring a channel outage, z. Then, Section III-B studies the retransmission statistics of HARQ-CC, developing approximations for $\bar{\tau}$ and $\bar{\tau}_{\text{out}}$ for both fast-fading and block-fading conditions.

Most of the results of this section are stated in terms of the FER. The relationship between the FER and the SER depends on the specific ECC used, and is addressed in Appendix B.

A. Simple HARQ (S-HARQ)

Let us first study the statistics of τ_{out}, defined in Section II-A5. Recall that, after an outage event is declared, the transmitter waits for at least one coherence time before performing further transmission attempts. If a transmission trial fails in S-HARQ then the received frame is discarded, as there is no reuse of that signal with earlier or later retransmissions [24]. This makes each transmission performed after an outage event independent of previous outage declarations. This implies, in turn, that outage declarations are independent of each other, and hence, that τ_{out} has a geometric distribution – i.e. its probability density function (p.d.f.) is given by

$$\mathbb{P}\{\tau_{\text{out}} = j\} = (1 - q_z) q_z^j \ , \tag{19}$$

where $\mathbb{P}\{\mathcal{A}\}$ denotes the probability of the event $\mathcal{A}$ and $q_z = 1 - \mathbb{P}\{\tau \leq z\}$ is the outage probability. Note that q_z does not require a time index because in S-HARQ the error statistics are stationary. By a direct calculation, the mean value of τ_{out} can be shown to be:

$$\bar{\tau}_{\text{out}} = \frac{q_z}{1 - q_z} \ . \tag{20}$$

Let us now study the statistics of τ. First, note that the p.d.f. of τ_z is given by (c.f. II-A5)

$$\mathbb{P}\{\tau_z = t\} = \mathbb{P}\{\tau = t | \tau \leq z\} = \frac{\mathbb{P}\{\tau = t\}}{1 - q_z} \ , \tag{21}$$

where t is an integer such that $t \leq z$. Its mean value is thus calculated as

$$\bar{\tau}_z = \sum_{t=1}^{z} t \cdot \mathbb{P}\{\tau_z = t\} = \frac{1}{1 - q_z} \sum_{t=1}^{z} t \cdot \mathbb{P}\{\tau = t\} \ . \tag{22}$$

Finally, by using (11), (20) and (22), it can be shown that the mean number of transmission trials is given by

$$\bar{\tau} = z\bar{\tau}_{\text{out}} + \bar{\tau}_z = \frac{1}{1-q_z}\left(zq_z + \sum_{t=1}^{z} t\mathbb{P}\{\tau = t\}\right) \quad . \tag{23}$$

The search of explicit expressions for (20) and (23) for specific channels and transmission schemes is carried out in the sequel.

1) Fast-fading case: Let us assume that the probabilities of frame error of successive transmission trials, $\left\{P_{\text{f}}^{\text{ff}}(1), P_{\text{f}}^{\text{ff}}(2), \dots\right\}$, are a set of i.i.d. random variables, whose mean value is denoted as $\bar{P}_{\text{f}}^{\text{ff}} := \mathbb{E}\{P_{\text{f}}^{\text{ff}}(1)\}$. Note that the i.i.d. assumption holds when a deep interleaver is used, which decorrelates the channel coefficients of successive symbols [25]. Then, using (69) from Appendix C, the outage probability under these conditions can be found to be

$$q_z^{\text{ff}} = \left(\bar{P}_{\text{f}}^{\text{ff}}\right)^z \quad . \tag{24}$$

From (24), along with the fact that $0 \leq \bar{P}_{\text{f}} < 1$, one can conclude that $q_{z+1}^{\text{ff}} < q_z^{\text{ff}}$. This, in combination with (20), shows that

$$\bar{\tau}_{\text{out}}^{\text{ff}}(1) \geq \bar{\tau}_{\text{out}}^{\text{ff}}(2) \geq \dots \lim_{z\to\infty} \bar{\tau}_{\text{out}}^{\text{ff}}(z) = 0 \quad . \tag{25}$$

Now, using (74) from Appendix C, the mean number of transmission trials can be calculated for this case to be[†]

$$\bar{\tau}^{\text{ff}}(z) = \frac{1}{1-\left(\bar{P}_{\text{f}}^{\text{ff}}\right)^z} \sum_{t=0}^{z-1} \left(\bar{P}_{\text{f}}^{\text{ff}}\right)^t \tag{26}$$

$$= \frac{1}{1-\bar{P}_{\text{f}}^{\text{ff}}} \quad . \tag{27}$$

This shows that $\bar{\tau}^{\text{ff}}(z)$ gives the same value for any choice of parameter z. This result, in combination with (29), reflects the intuitive fact that nothing is won in a fast fading scenario by waiting in sleep mode for new channel realizations. Because of this, in the rest of this work it will be assumed that for fast-fading schemes $z = \infty$ and hence $\bar{\tau}_{\text{out}}^{\text{ff}} = 0$.

2) Block-fading case: Consider now a static channel, where the frame error probabilities, defined now as $\left\{P_{\text{f}}^{\text{bf}}(1), P_{\text{f}}^{\text{bf}}(2), \dots\right\}$, are fully correlated and hence $P_{\text{f}}^{\text{bf}}(t) = P_{\text{f}}^{\text{bf}}(1)$ for all $t \in \{1, \dots, z\}$. Note that in this case all the symbols that compose a frame undergo channel fading with the same channel realization, in contrast to the fast-fading scenario where each symbol experiences an independent channel realization.

[†]Both (27) and (33) correspond to equivalent expressions reported in [4] for the case where $z = \infty$.

Under these assumptions, the outage probability can be found using (69) in the Appendix C to be

$$q_z^{\text{bf}} = \mathbb{E}\left\{\left(P_{\text{f}}^{\text{bf}}\right)^z\right\} \quad , \tag{28}$$

where $P_{\text{f}}^{\text{bf}} := P_{\text{f}}^{\text{bf}}(1)$ is just a shorthand notation. Following an analysis similar to the one presented in Section III-A1, one can conclude that $q_{z+1}^{\text{bf}} < q_z^{\text{bf}}$ and therefore

$$\bar{\tau}_{\text{out}}^{\text{bf}}(1) \geq \bar{\tau}_{\text{out}}^{\text{bf}}(2) \geq \ldots \lim_{z\to\infty} \bar{\tau}_{\text{out}}^{\text{bf}}(z) = 0 \ . \tag{29}$$

also holds.

The mean number of transmission trials for block-fading channels can be calculated using (28) with (74) from Appendix C:

$$\bar{\tau}^{\text{bf}}(z) = \frac{1}{1-\mathbb{E}\left\{\left(P_{\text{f}}^{\text{bf}}\right)^z\right\}}\mathbb{E}\left\{\sum_{t=0}^{z-1}\left(P_{\text{f}}^{\text{bf}}\right)^t\right\} \tag{30}$$

$$= \frac{1}{1-\mathbb{E}\left\{\left(P_{\text{f}}^{\text{bf}}\right)^z\right\}}\mathbb{E}\left\{\frac{1-\left(P_{\text{f}}^{\text{bf}}\right)^z}{1-\left(P_{\text{f}}^{\text{bf}}\right)}\right\} \ . \tag{31}$$

It is interesting to notice that, for the case with $z = 1$, one can show that

$$\bar{\tau}^{\text{bf}}(1) = \bar{\tau}_{\text{out}}^{\text{bf}}(1) + 1 \ . \tag{32}$$

This is a consequence of (20), (28) and (31), and is consistent with the fact that, when $z = 1$, then each decoding error corresponds to an outage declaration.

In Appendix D we show that $\bar{\tau}^{\text{bf}}(z)$ is an increasing function of z, and hence $\bar{\tau}^{\text{bf}}(1) \leq \bar{\tau}^{\text{bf}}(2) \leq \cdots \leq \bar{\tau}_{\infty}^{\text{bf}}$. Therefore, by performing fewer transmission trials per coherence time (i.e. small z), the system can exploit a diversity gain that improves the retransmission statistics, albeit at the cost of decreasing the overall throughput. The last term of the succession can be expressed as

$$\bar{\tau}_{\infty}^{\text{bf}} = \lim_{z\to\infty}\bar{\tau}^{\text{bf}}(z) = \mathbb{E}\left\{\frac{1}{1-P_{\text{f}}^{\text{bf}}}\right\} \quad , \tag{33}$$

which is an upper-bound $\bar{\tau}^{\text{bf}}(z)$ for all z. Note that, above, the last equality can be rigorously derived using the Lebesgue's dominated convergence theorem [26] (which can be applied because the condition $0 \leq P_{\text{f}}^{\text{bf}} \leq 1$ implies $\left(P_{\text{f}}^{\text{bf}}\right)^t \geq \left(P_{\text{f}}^{\text{bf}}\right)^{t+1}$).

B. HARQ with Chase combining (HARQ-CC)

The idea of Chase combining is to use the information contained in previous transmission attempts for reducing the outage probability [27]. Concretely, if the received signal for the

symbol s during the t-th transmission trial has the form $y_t = h_t s + w_t$, where h_t is the narrowband complex baseband equivalent channel coefficient and w_t is the corresponding baseband equivalent additive white Gaussian noise term, then the u-th decoding of s is done using maximum ratio combining (MRC, c.f. [25]) of all previous observations $y_1, \ldots, y_u$, i.e.

$$\tilde{y}_u = \sum_{t=1}^{u} h_t^* y_t \tag{34}$$

$$= \left(\sum_{t=1}^{u} |h_t|^2 \right) s + \sum_{t=1}^{u} h_t^* w_t \tag{35}$$

$$:= \tilde{h}_u s + \tilde{w}_u \ . \tag{36}$$

In the following, it is assumed that the channel coefficients h_t follow the Nakagami-m fading model [28]. This fading distribution is convenient because it is both mathematically tractable and covers the entire range of fading scenarios from AWGN ($m \to \infty$) to Rayleigh fading ($m = 1$) [29]. The squared magnitude of a Nakagami-m fading channel $|h|^2 = r$ is a Gamma random variable $\Gamma(m, \mu)$, whose p.d.f. is given by

$$f_{\mu,m}(r) = \left(\frac{m}{\mu} \right)^m \frac{r^{m-1}}{\Gamma(m)} \exp\left(-\frac{mr}{\mu} \right) \ . \tag{37}$$

Above, μ is the mean power gain and m is the diversity gain of the channel [29].

A direct calculation on (36) shows that the SNR at the output of the MRC combiner after the u-th transmission trial is given by

$$\gamma_u = \sum_{t=1}^{u} |h_t|^2 \bar{\gamma} \ , \tag{38}$$

where $\bar{\gamma} = E_\mathrm{s}/N_0$, with E_s the symbol energy and N_0 the noise power spectral density. Above, each $|h_t|^2$ is a Gamma random variable with parameters $\mu = 1$ and m. An analysis of the cases of fast-fading and block-fading scenarios is provided in the sequel.

1) Fast-fading case: In a fast-fading scenario the terms $|h_t|^2$ of (38) are i.i.d. Gamma random variables. By a standard argument involving the product of characteristic functions, it can be shown that γ_u in this case is also Gamma distributed with parameters $m_u = u \cdot m$ and $\mu_u = u \cdot \bar{\gamma}$. Therefore, if $P_M(\gamma)$ denotes the symbol error rate (SER) of a given M-QAM modulation with SNR γ, then the mean SER when looking at the output of the MRC combiner is given by

$$\bar{P}_\mathrm{M}^{\mathrm{cc,ff}}(u) = \int_0^\infty P_M(\gamma_u) f_{u\bar{\gamma},um}(\gamma_u) \mathrm{d}\gamma_u \tag{39}$$

$$:= \bar{P}_M(u\bar{\gamma}, um) \ , \tag{40}$$

with $f_{u\bar{\gamma},um}(\gamma)$ as defined in (37). This shows that Chase combining yields both a power gain and a diversity gain proportional to the number of transmission attempts.

Let us denote $\tau^{\text{cc,ff}}$ as the number of transmission trials of Chase combining over a fast-fading channel. By inspecting (35), it can be seen that the combined channel coefficients $\tilde{h}_u$ and noise terms $\tilde{w}_u$ (c.f. (36)) for different values of u are correlated. However, simulations show that the correlation becomes negligible for sufficiently long frames (e.g. more than 100 symbols). This "randomization" is a consequence of the large number of new independent random variables which are involved in each new transmission trial (one channel and one noise per symbol). Therefore, one can use the following approximation for the p.d.f. of $\tau^{\text{cc,ff}}$ for transmissions over a Nakagami-m channel:

$$\mathbb{P}\{\tau^{\text{cc,ff}}=t\}\begin{cases}=1-\bar{P}_{\text{f}}^{\text{cc,ff}}(1) & \text{for } t=1\\ \approx[1-\bar{P}_{\text{f}}^{\text{cc,ff}}(t)]\prod_{u=1}^{t-1}\bar{P}_{\text{f}}^{\text{cc,ff}}(u) & \text{for } t\geq 2\end{cases} \tag{41}$$

where $\bar{P}_{\text{f}}^{\text{cc,ff}}(u)$ denotes the FER over a Nakagami-m_u channel with power gain $\mu_u = u\cdot\bar{\gamma}$, like the one discussed above. Recalling that there is no reason for imposing an upper bound on the number of retransmissions in a fast-fading scenario (c.f. III-A1), one can show that

$$\bar{\tau}^{\text{cc,ff}} = \sum_{t=1}^{\infty} t\cdot\mathbb{P}\{\tau^{\text{cc,ff}}=t\} \tag{42}$$

$$\approx 1+\sum_{t=1}^{\infty}\prod_{u=1}^{t}\bar{P}_{\text{f}}^{\text{cc,ff}}(u)\ . \tag{43}$$

Above, (42) is obtained using the definition of the expected value operator, and (43) is obtained by using (41) and some straightforward algebra. Is to be noted that if no limit for the number is retransmissions is assumed (i.e. $z=\infty$), then $\bar{\tau}_{\text{out}}^{\text{cc,ff}}=0$ (c.f. Section III-A1).

By taking (43) as an equality, one can prove that HARQ-CC outperforms S-HARQ in a fast-fading scenario in the sense that $\bar{\tau}^{\text{cc,ff}}\leq\bar{\tau}^{\text{ff}}$. In effect, $\bar{P}_{\text{f}}^{\text{cc,ff}}(u)\leq\bar{P}_{\text{f}}^{\text{cc,ff}}(1)=\bar{P}_{\text{f}}$ for any positive integer u due to the combining benefits of CC. By using this inequality for each $u=1,\ldots,t$, one can show that

$$\prod_{u=1}^{t}\bar{P}_{\text{f}}^{\text{cc,ff}}(u)\leq\left(\bar{P}_{\text{f}}\right)^{t}\ . \tag{44}$$

Finally, the desired result follows from comparing (27) and (43), and noticing that the former can be rewritten as $\bar{\tau}^{\text{ff}}=\sum_{t=0}^{\infty}\bar{P}_{\text{f}}^{t}$.

2) Block-fading case: Let us consider now the case of a block-fading scenario, where the fading coefficients h_t (c.f. (34)) that belong to the same coherence time interval are equal, while coefficients from different coherence times are independent. One may divide the number of transmission trials u as $u = vz + x$, where z is as defined in Section II-A5, $v \geq 0$ is the number of previous channel coherence time intervals in which transmission attempts have been run and $x \in \{1, \dots, z-1\}$ is the trial index within the current run of transmissions. Then, for the case of block fading one finds that (38) can be re-written as

$$\gamma_{vz+x} = \left(x|h_{v+1}|^2 + z \sum_{i=1}^{v} |h_i|^2 \right) \bar{\gamma} \ , \tag{45}$$

where the index i represents the coherence time. This shows that although each retransmission provides a power gain (as $\bar{\gamma}_{vz+x} = (vz+x)\bar{\gamma}$ for any value of v and x), only transmissions performed on different coherence times provides diversity.

Let us focus on the case of $z = 1$ (i.e. $u = v$ and $x = 0$), which is the setup that gives the highest diversity gain for a given number of transmission trials. Under these conditions, it can be seen from (45) that during the u-th trial each transmitted symbol experiences a SNR that corresponds to a Nakagami-m_u channel with $m_u = u \cdot m$ and power gain $\mu_u = u \cdot \bar{\gamma}$. As each decoding error causes an outage declaration, this case has a similar SER than the fast-fading case (c.f. (39)). Nevertheless, the FER is different because the whole frame experience the same channel coefficient, while in the fast fading case symbol of the same frame experience independent channel realizations (c.f. Section III-A2). As a consequence, the randomization argument that leads to (41) is not valid in this case. However, the thermal noise coefficient that corresponds to each received symbol is independent, and simulations show that a for sufficient large frame length (more than 100 symbols) a randomization still happens with respect to the noise conditioned on the channel realization. This allows us to use the following approximation:

$$\mathbb{P}\{\tau^{\text{cc,bf}} = t|\boldsymbol{h}\} \begin{cases} = 1 - P_{\text{f}}^{\text{cc,bf}}(\gamma_1) & \text{for } t = 1 \\ \approx [1 - P_{\text{f}}^{\text{cc,bf}}(\gamma_t)] \prod_{u=1}^{t-1} P_{\text{f}}^{\text{cc,bf}}(\gamma_u) & \text{for } t \geq 2 \end{cases} \tag{46}$$

where $\boldsymbol{h} = (h_1, h_2, \dots)$ is the vector of successive channel realizations, $P_{\text{f}}^{\text{cc,bf}}(\gamma)$ is the block-fading FER of an AWGN channel with SNR γ and γ_u is the SNR of the u-th decoding trial, which is calculated from $\boldsymbol{h}$ using (38). Then, using (46) and the fact that $\mathbb{P}\{\tau^{\text{cc,bf}} = t\} =$

$\mathbb{E}\left\{\mathbb{P}\{\tau^{\text{cc,bf}} = t|\boldsymbol{h}\}\right\}$, a direct calculation shows that

$$\bar{\tau}^{\text{cc,bf}} = \sum_{t=1}^{\infty} t\mathbb{E}\left\{\mathbb{P}\{\tau^{\text{cc,bf}} = t|\boldsymbol{h}\}\right\} \tag{47}$$

$$\approx \sum_{t=1}^{\infty} t\mathbb{E}\left\{\prod_{u=1}^{t-1} P_{\text{f}}^{\text{cc,bf}}(\gamma_u) - \prod_{v=1}^{t} P_{\text{f}}^{\text{cc,bf}}(\gamma_v)\right\} \tag{48}$$

$$= 1 + \sum_{t=1}^{\infty} \mathbb{E}\left\{\prod_{u=1}^{t} P_{\text{f}}^{\text{cc,bf}}(\gamma_u)\right\} \ . \tag{49}$$

Finally, it should be noted that (19) is not valid in the case of HARQ-CC, as the combination of old transmission trials make the outage probability smaller in each new coherence time. Therefore, in this case $\bar{\tau}_{\text{out}}^{\text{cc,bf}}$ does not distribute as a geometric random variable. Nevertheless, for the case of $z = 1$ then the arguments that lead to (32) are still valid, and therefore one can compute $\bar{\tau}_{\text{out}}^{\text{cc,bf}}$ using the following relationship:

$$\bar{\tau}_{\text{out}}^{\text{cc,bf}} = \bar{\tau}^{\text{cc,bf}} - 1 \ . \tag{50}$$

IV. Optimality analysis

In this section we consider the optimization problem of finding the values of the SNR, modulation size, code rate and retransmission scheme that allow for achieving the most energy-efficient data transmission. First, based on results presented in Section III, Section IV-A studies the optimization of the SNR. Then, Section IV-B analyzes the optimization of the code rate, the modulation size and the retransmission scheme. The theoretical results derived in these subsections are illustrated by the simulation presented in Section V.

A. Optimization of the SNR

Consider our energy model as stated by (17). Using (20), (17) can be re-written as

$$\bar{\mathcal{E}}_{\text{b}} = \frac{2\mathcal{E}_{\text{st}} q_z}{1 - q_z} + \mathcal{E}_{\text{enc}} + (P_{\text{eff}} + Ad^{\alpha}\bar{\gamma})T\bar{\tau} \ , \tag{51}$$

where $P_{\text{eff}} = P_{\text{el}} + \mathcal{E}_{\text{dec}}/T$. A direct inspection of (51) reveals that the energy consumption of a given transmission scheme is large at extreme values of the total SNR. In effect, low values of SNR are not energy-efficient, because a large number of retransmissions are required for achieving a correctly decoded frame in the receiver —which is reflected in large values of $\bar{\tau}$ and q_z. On the other hand, high values of SNR are not efficient either, because they involve a large power consumption of the PA, which is proportional to $\bar{\gamma}$ (c.f. Section II-A2).

Moreover, it can be shown that there exists a unique optimal SNR between these two extremes, which represents the most favorable trade-off between irradiated power and consumption due to retransmissions. Note first that q_z, as derived in Section III, is expressed as a combination of sums (averages) and products of FERs, and therefore it can be shown to be a convex function of the mean SNR. In fact, this can be done by taking into account the convexity of the FER (which is inherited from the convexity of the SER) and the fact that the product of positive non-increasing convex functions is also convex [30, Ex. 3.23]. Using a similar rationale, it can also be shown that the expressions found for $\bar{\tau}$ for HARQ-CC (c.f. Section III-B) are convex. Finally, the expressions presented for S-HARQ in (27) and (30) share a similar structure, namely, they are the product of two functions: a combination of products and sums of FERs (and hence convex), and the reciprocal of one minus such a combination. The later is the composition of a non-decreasing function (the reciprocal) and a concave function, and is therefore also convex [30, Ch. 3]. Hence, for S-HARQ $\bar{\tau}$ is the product of two non-negative non-increasing convex functions of the mean SNR and hence it is also convex. Finally, following a similar argument one can also show that $q_z/(1-q_z)$ is a convex of the mean SNR too.

The above discussion shows that $\bar{\mathcal{E}}_{\text{b}}$ is a convex function of $\bar{\gamma}$, and therefore the optimal SNR $\bar{\gamma}^*$ is the unique value of $\bar{\gamma}$ such that $\partial\bar{\mathcal{E}}_{\text{b}}/\partial\bar{\gamma}(\bar{\gamma}^*) = 0$. Using this condition on (51), one can find the following implicit equation for $\bar{\gamma}^*$:

$$\frac{a}{[1-q_z]^2}\frac{\partial q_z}{\partial\bar{\gamma}}(\bar{\gamma}^*) + [b+\bar{\gamma}^*]\frac{\partial\bar{\tau}}{\partial\bar{\gamma}}(\bar{\gamma}^*) + \bar{\tau} = 0 \ , \tag{52}$$

where $P_{\text{st}} = 2\mathcal{E}_{\text{st}}/T$, $a = P_{\text{st}}/(Ad^{\alpha})$ and $b = P_{\text{eff}}/(Ad^{\alpha})$. Note that the factor Ad^{α} represents the power consumption of the PA, so a and b are related to the ratio between the PA power consumption and the startup and baseband consumption, respectively. It is interesting to notice that the optimal SNR depends only on q_z, $\bar{\tau}$, a and b.

It is insightful to study (52) for extreme values of the link distance. Indeed, by noting that $a, b \propto d^{-\alpha}$, it can be seen that if $d \to 0$ then $a, b \to \infty$ and hence (52) can be re-written as

$$\frac{\partial}{\partial\bar{\gamma}}\left\{\frac{q_z}{1-q_z} + \delta\bar{\tau}\right\} = 0 \ , \tag{53}$$

where $\delta = b/a = P_{\text{eff}}/P_{\text{st}}$ measures the ratio between the baseband and startup power consumption. Note that $q_z/(1-q_z)$ is a decreasing function of $\bar{\gamma}$ because q_z is also so. As $\bar{\tau}$ is also decreasing on $\bar{\gamma}$, then the left hand side term of (53) represents the slope of a positive and decreasing function (the whole term inside the brackets) whose value tends to a constant

(δ) monotonically as $\bar{\gamma}$ grows. Hence, the optimal SNR is a value of $\bar{\gamma}$ high enough such that $\bar{\tau} \approx 1$ and $q_z \approx 0$ holds, as then the term inside brackets in (53) is practically a constant.

On the other hand, if $d \to \infty$ then $a, b \to 0$, and hence (52) can be re-written as

$$\frac{\partial \log \bar{\tau}}{\partial \bar{\gamma}} (\bar{\gamma}^*) = -\frac{1}{\bar{\gamma}^*} \quad . \tag{54}$$

Therefore, in this case the optimal SNR only depends on the shape of the $\bar{\tau}(\bar{\gamma})$ curve, being indifferent to electronic or baseband consumption terms.

Finally, it can be shown that the optimal SNR for large distances is smaller than the optimal SNR for short ones. In effect, from the discussion after (53) is clear that for long transmission distances the slope of $\bar{\tau}$ at the optimal SNR, and hence also the slope of $\log \bar{\tau}$[‡], has to be approximately zero. On the other hand, (54) shows that the slope of $\log \bar{\tau}$ evaluated at the optimal SNR for short transmission distances is strictly negative. Note that $\log \bar{\tau}$ decreases monotonically to 1 as the SNR grows, and hence its slope is always negative but increases towards zero as SNR $\to \infty$. Hence, our claim follows from the fact that a slope closer to zero implies a larger SNR.

B. Qualitative Analysis of the Optimization for Long and Short Range Transmissions

Let us denote as $\bar{\mathcal{E}}_{\mathrm{b}}^*$ the energy consumption when the optimal SNR $\bar{\gamma}^*$ is being used. In the following, $\bar{\mathcal{E}}_{\mathrm{b}}^*$ is studied for both large and small values of the link distance. For simplicity of the analysis we consider no throughput constraints. However, the inclusion of such constraints represent a straightforward extension of the presented framework that can be done by introducing additional restrictions on the space of parameters.

1) Long range transmissions: When the link distance is large, then the consumption of the PA dominates over the consumption of electronic components. Hence, (51) can be approximated as

$$\bar{\mathcal{E}}_{\mathrm{b}}^* \approx A d^{\alpha} \bar{\gamma}^* T \bar{\tau} (\bar{\gamma}^*) \quad . \tag{55}$$

Let us recall that, for the case of long range communications, $\bar{\gamma}^*$ only depends on the shape of $\bar{\tau}$ as function of the SNR. Therefore, communication schemes with favorable error statistics are an interesting alternative to explore, as they provide a $\bar{\tau}$ curve which when plugged in (54) defines a low optimal SNR. This means, in connection to (55), that these schemes are

[‡]Note that as $\bar{\tau} \geq 1$ then $\frac{\partial \log \bar{\tau}}{\partial \bar{\gamma}} = \frac{1}{\bar{\gamma}} \frac{\partial \bar{\tau}}{\partial \bar{\gamma}} \leq \frac{\partial \bar{\tau}}{\partial \bar{\gamma}}$.

optimal for this case as they achieve a reduced number of retransmission while requiring only a moderate PA consumption.

From the above discussion one can conclude that, when performing long range transmissions, HARQ-CC is a good choice from an energy point of view, as it allows for improving the error statistics while keeping all the other terms in (55) constant. Also small modulations are attractive for this case, as they further improve the error statistics and hence decrease $\bar{\gamma}^*$ (as in this case $\bar{\gamma}^*$ only depends on $\bar{\tau}$) at the cost of a slight increase in T (c.f. Section II-A1). On the other hand, the optimization of the code rate is less straightforward: while a lower code rate also improves the error statistics, it causes a significant increase of the total time per bit ($T \propto r^{-1}$, c.f. (1)). Therefore, reducing the code rate is only profitable if the benefit of reducing the optimal SNR is larger than the loss for increasing the transmission time due to the added redundancy.

2) Short range transmissions: In Section IV-A, it was shown that the optimal SNR conditions for short range transmissions imply $q_z \approx 0$ and $\bar{\tau} \approx 1$. Hence, (51) can be approximated in this case as

$$\bar{\mathcal{E}}_{\text{b}} \approx 2\mathcal{E}_{\text{st}} + \mathcal{E}_{\text{enc}} + P_{\text{eff}}T \ . \tag{56}$$

From above is apparent that in this case the consumption of the PA becomes negligible compared to the cost of the baseband electronic components. Therefore, under these circumstances simple transmission schemes are attractive, as they have small encoding and decoding costs. HARQ-CC and low code rates are not a good choice for this case, as they increase $\mathcal{E}_{\text{enc}}$, P_{eff} and/or T without providing substantial benefits. On the contrary, large modulation constellations are desirable as they reduce T by packing many bits in each transmitted symbol.

V. Analysis of Chase Combining with BCH and Convolutional Codes

In this section we study the energy consumption of systems that use BCH or convolutional codes with S-HARQ or HARQ-CC. These coding schemes were selected because of two reasons: they are simple codes with a straightforward and viable implementation in low power devices, and they are flexible enough to provide a good range of different code rates. For the convolutional codes, we consider the regular codes of rate $1/n$ from [32], and the punctured convolutional codes of rate k/n for $k > 1$ from [33]. The former are optimum codes in terms of distance spectrum, while the latter are good codes in terms of distance spectrum but with considerably reduced complexity when compared to regular codes of the

same rate. For the BCH codes we consider the 106 codes with $n = 1023$, whose code rates range from 1 to 0.01[§].

For each transmission scheme the minimal energy consumption per bit is computed for various link distances. This is achieved by optimizing the code rate, the irradiated power and the size of the modulation constellation. The optimization of the modulation order was done considering BSPK, QPSK and M-QAM with $M \in \{8, 16\}$. The optimization of the irradiated power was performed considering an upper irradiation power limit of 10 mW, which is a common assumption for WSN [31]. For computing (17) we used parameters of state-of-the-art low-power devices, which are listed in Table II. Finally, for the cost of computations we considered a dedicated APU with $c_{\text{add}} = c_{\text{prod}} = c_{\text{int-comp}} = c_{\text{bin-comp}} = 1$ (c.f. Section II-A4).

TABLE II: Generic low-power device parameters

Parameter	Description	Value
L_{P}	Payload length	1023 bits
L_{H}	Frame Header	2 bytes *
L_{O}	Overhead	5 bytes *
L_{F}	Feedback frame length	11 bytes *
W	Bandwidth	1 MHz §
R_{s}	Symbol rate	125 kBaud §
T_{st}	Wake-up time	20 mS †
α	Path-loss coefficient	3.2 *
A_0	Free space path loss	30 dB *
η	PA efficiency	0.785 ||
$P_{\text{el,tx}}$	Tx electronic power consumption	11.2 mW ††
$P_{\text{el,rx}}$	Rx electronic power consumption	16.6 mW ††
N_0	Noise power density	-174 dBm/Hz
N_{f}	Receiver noise figure	4.4 dB ††
M_{l}	Link margin	30 dB *
f_{APU}	APU frequency	20 MHz ‡
V_{dd}	APU voltage	3 V ‡
I_0	Average current	6.37 mA ‡

*source: [4], §source: [34], †source: [35], ‡source: [36], ||source: [37], ††source: [38].

Results obtained for a block fading scenario are presented in Figures 2 through 6, where uncoded S-HARQ transmissions with $z = 3$ transmission trials per coherence time are

§The complete list of BCH codes for various values of n can be found in [40].

compared with coded transmissions with S-HARQ and HARQ-CC considering $z = 3$ and $z = 1$. The curves consider Nakagami-m fading with $m = 1$, which is equivalent to Rayleigh fading and corresponds to the case of non line-of-sight links, reason for which this scenario demands the highest number of retransmissions (simulations for fast-fading channels where also performed, but the results are not discussed here due to lack of space).

The results for each retransmission scheme confirm the following general principle, already discussed in Section IV-B and found as well in [39]: *for long-range transmissions the optimal schemes are the ones with high diversity gain, while for short link distances the best are schemes with a large multiplexing gain* (see Figure 1). This means that, for each retransmission scheme, the best configuration for performing long range transmissions is an computationally expensive code with a low code rate and a low order M-ary constellation; for the studied cases, this means BPSK with convolutional codes (see Figures 2 and 3). On the other hand, the most efficient solution for a short transmission range is to use codes with high rate and large constellation orders —i.e. higher net throughput. In our case, this means 16-QAM with a BCH code with a high rate, or even uncoded transmissions for really short link distances. Results also show that the optimal SNR decreases when the link distance grows, confirming the discussion presented in Section IV-A (see Figure 4). Moreover, it is worth noting that the optimal code rate decreases as the link distance grows for all the studied retransmission schemes (see Figure 2), in agreement with the discussion presented in Section IV-B. Nevertheless, the code rate drops slower in CC-HARQ than in the S-HARQ case because of the retransmission statistics improvement delivered by the HARQ-CC diversity gain (see Figure 5).

Following the same rationale, and also in agreement with Section IV-B, HARQ-CC transmissions are significantly more efficient than S-HARQ transmissions when the link distance is large (see Figure 1). In fact, the choice of the HARQ scheme has a stronger effect on the energy consumption than the choice of the ECC, as the diversity gain introduced by HARQ-CC allows for a more graceful degradation of the performance as the link distance increases. This, in turn, significantly extends the transmission range of a low-power communication device. In contrast to plain error correction coding (i.e. S-HARQ), Chase combining improves the error rates without introducing redundant bits (and therefore increasing the effective air time per bit), and also without incurring in important additional computational costs. In fact, it is interesting to observe that the decoding costs can dominate the overall energy-budget for large link distances (see Figure 6).

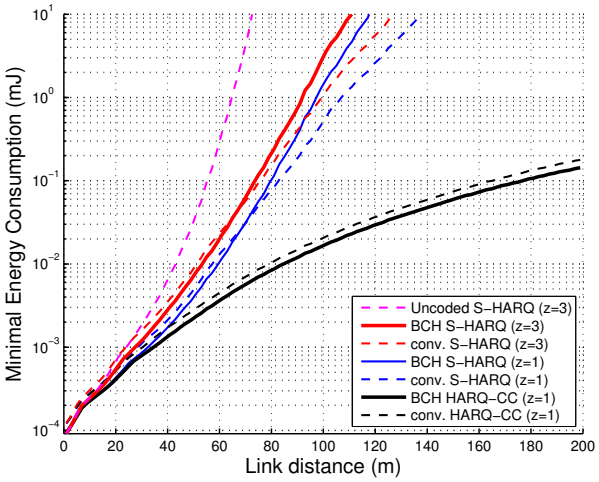

Fig. 1: Minimum energy consumption per goodbit when the SNR, the modulation scheme and the coding rate are optimized for each link distance. The energy efficiency is clearly impacted stronger by the chosen HARQ scheme than by the error correcting code choice.

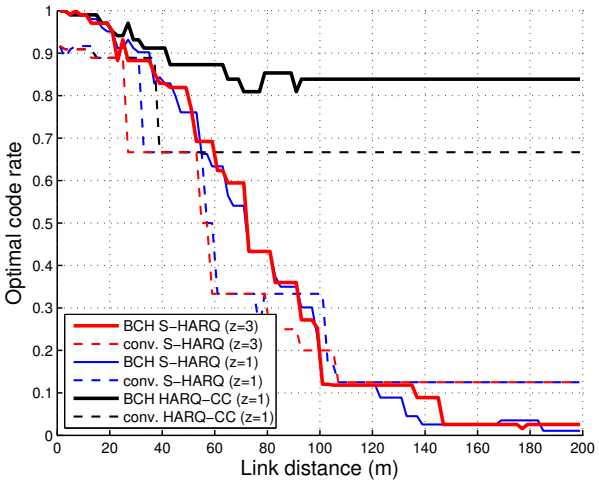

Fig. 2: The code rate at which the amount of introduced redundancy allows for achieving maximal energy-efficiency. Low code rates are a good choice for long link distances because the code gain allows to achieve a target bit error rate radiating less power, while they are suboptimal for short range communications because the higher time per bit increases the consumption of the electronic components.

VI. Conclusion

We studied the effects of error correcting codes and HARQ retransmission schemes on the average energy required for delivering one bit of data without error over a wireless communication link. The analysis considered the consumption of electronic components of the transceiver, the cost of the computations required for encoding and decoding the data

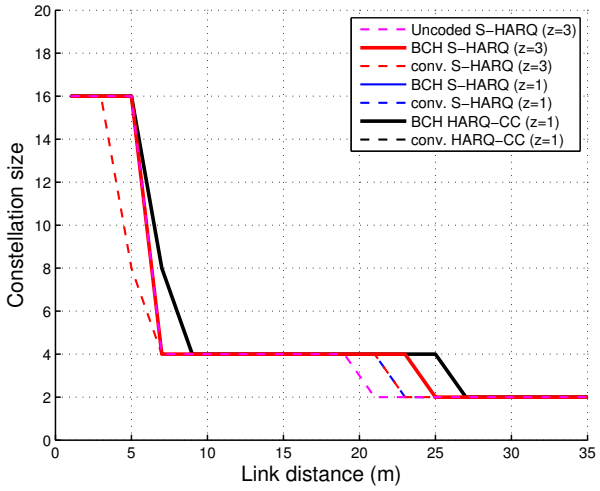

Fig. 3: Optimal order of an M-ary constellation. Modulations with higher throughput are more energy-efficient when the link distance is short, while schemes with lower throughput but better error statistics are optimal for long range transmissions.

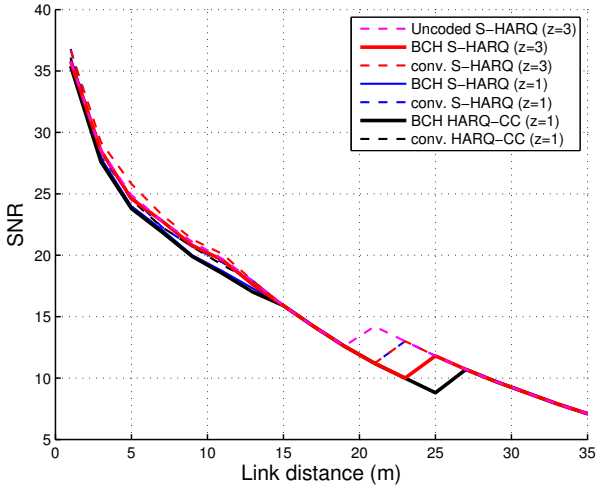

Fig. 4: Optimal SNR, which relates directly to the level of irradiated power that achieves the most energy-efficient balance between radiated power and number of retransmissions. Note that the discontinuities that exist correspond to changes in the optimal modulation (c.f. Figure 3).

and the effects of retransmissions due to decoding errors that are beyond the correcting capabilities of the code. We derived expressions for the mean number of transmission trials for simple HARQ and HARQ with Chase combining for fast-fading and block-fading scenarios under Nakagami-m channel fading statistics. We showed that diversity is in general beneficial between successive transmission trials.

We found that HARQ-CC and codes with low code rates are better suited for long range

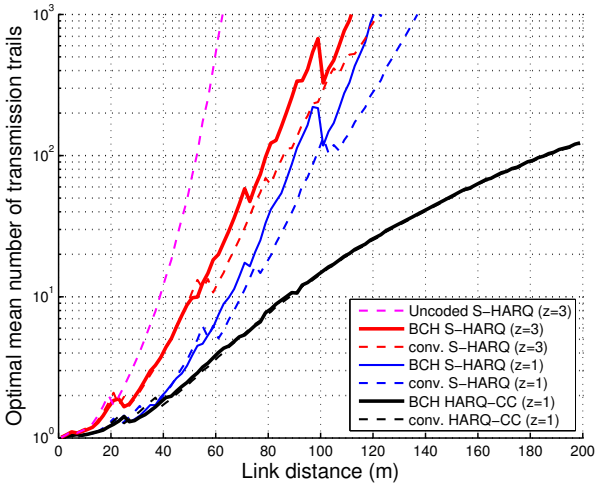

Fig. 5: HARQ-CC can achieve a lower number of retransmissions over a wider range of distances, while keeping a low power consumption at the PA. This is a consequence of the significant error-rate improvements provided by the diversity gain of this scheme.

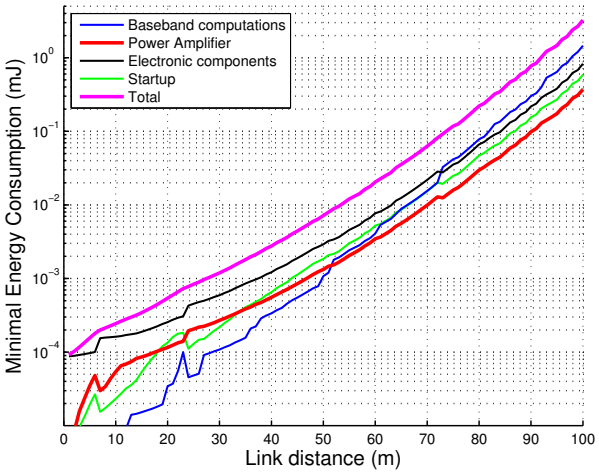

Fig. 6: Decomposition of the energy consumption sources of S-HARQ with BCH coding over a block-fading channel, using $z = 3$ transmission trials per coherence time period. The decoding cost — of codes with low code rate (see Figure 2)— dominates the overall energy budget when the link distance is large.

transmissions, as they attain low error rates with less irradiated power. On the other hand, S-HARQ and high code rates are optimal for short range transmissions, because they reduce the computational load and the average air time spent per data bit which are relevant when the irradiated power is not dominant. Moreover, we found that the choice of the retransmission scheme impacts strongly the energy efficiency than the choice of ECC scheme.

Finally, we found that using HARQ-CC significantly extends the transmission range of a

low-power communication devices compared to S-HARQ, because the more favorable error statistics allow for a more graceful degradation of the performance as the link distance increases.

APPENDIX A
COSTS OF ENCODING AND DECODING

In the following, we analyze the encoding and decoding operations of BCH and convolutional codes of rate $r = k/n$ that can correct up to t_{c} errors per codeword of $n = L_{\mathrm{P}}$ bits. All the results for BCH codes and convolutional codes are summarized in Table I. In the case of linear codes, is to be noted that choosing $n < L_{\mathrm{P}}$ (so that there is more than one codeword per frame) does not bring additional gains in terms of energy efficiency [19]. Therefore, and for the sake of conciseness, we opted to present only the case of $n = L_{\mathrm{P}}$.

A. BCH codes

Let us assume an generator polynomial encoding strategy and a syndrome decoder [40]. Then, the number of required operations for encoding is at most $kL_{\mathrm{P}} - k^2$ binary additions, while decoding takes $(2L_{\mathrm{P}} - 1)t_{\mathrm{c}} + 2t_{\mathrm{c}}^2$ additions and $2L_{\mathrm{P}}t_{\mathrm{c}} + 2t_{\mathrm{c}}^2$ multiplications over a Galois Field (GF). If $L_{\mathrm{P}} = 1023$ as in Section V, the operations for decoding are over GF(2^{10}), which leads to $\mathcal{E}_{\mathrm{dec}} \gg \mathcal{E}_{\mathrm{enc}}$. Because of this, the term $\mathcal{E}_{\mathrm{enc}}$ is neglected within the simulation presented in Section V.

B. Convolutional codes

As in the case of BCH codes, encoding is not taken into account as it is considerably less complex than decoding. For decoding, a Viterbi algorithm (VA) with hard decision is considered in the following [40].

Let us consider a convolutional code of rate $r = k/n$ where k is the number of binary inputs, n is the number of binary outputs[¶], and ν is the memory order [41]. The total number of operations per frame required by the VA for decoding a regular (non-punctured) convolutional code are $L_{\mathrm{P}}2^{k+\nu}$ binary comparisons and integer additions and $L_{\mathrm{P}}2^{\nu}(2^k - 1)/n$ integer comparisons [42]. This shows that the complexity of the VA grows exponentially with the code rate. Puncturing [40] is an alternative for reducing the decoding complexity of high

[¶]Note that, differently than in the case of BCH codes, for convolutional codes n is typically much smaller than L_{P}.

rate convolutional codes, while keeping a good error performance. In the case of punctured convolutional codes, the total number of operations per frame required by the VA are [42] $L_{\mathrm{P}}2^{\nu+1}$ binary comparisons and $n_{\text{int-comp}} = rL_{\mathrm{P}}2^{\nu}$ integer comparisons.

C. Cost of HARQ-CC

With respect to S-HARQ, the computations required for HARQ-CC require two additional steps: (i) combining the symbols of the u transmission attempts of the frame and (ii) calculating the equivalent channel coefficient. For soft-combining the symbols of u transmission attempts, u multiplications and $u-1$ additions per symbol are carried out, which is valid for both fast fading and block fading channels (c.f. (34)). Then, for calculating the equivalent channel coefficient ($\tilde{h}_u$), $u-1$ additions per symbol are required in the case fast fading channel, while only $u-1$ additions are required for the whole frame in the case of block fading.

It is useful to adopt the following approximation for the total number of additions per transmission trial (c.f. Section II-B) over fast- and block- fading channels:

$$n_{\text{add}}^{\text{HARQ,ff}} = \frac{2(u-1)}{u} L_{\mathrm{P}} \approx 2L_{\mathrm{P}}, \tag{57}$$

$$n_{\text{add}}^{\text{HARQ,bf}} = \frac{(u-1)}{u}(L_{\mathrm{P}}+1) \approx L_{\mathrm{P}}+1 \ . \tag{58}$$

This implies a slight overestimation, which is anyway clouded by the higher costs of the ECC schemes. All this is summarised in Table I.

APPENDIX B
FER OF BCH AND CONVOLUTIONAL CODES

In the sequel, the FER calculations for both BCH and convolutional codes are presented.

A. BCH codes

Let us assume that $n = L_{\mathrm{P}}$, so that there is a single codeword per payload. Given the error correcting capability t_{c} of the code, the FER P_{f} can be written in terms of the bit error rate of the M-ary modulation used for the payload, $P_{\mathrm{b}}(\gamma)$, and of the binary modulation used for the header, $P_{\text{bin}}(\gamma)$, as [19]

$$P_{\mathrm{f}}(\gamma) = 1 - [1 - P_{\text{bin}}(\gamma)]^{H} \left[\sum_{j=0}^{t_{\mathrm{c}}} \binom{L_{\mathrm{P}}}{j} [1 - P_{\mathrm{b}}(\gamma)]^{L_{\mathrm{P}}-j} P_{\mathrm{b}}(\gamma)^{j} \right] \ . \tag{59}$$

B. Convolutional codes

In the case of convolutional codes with hard decision decoding, one can write the FER as

$$P_{\mathrm{f}}(\gamma) = 1 - \left[1 - P_{\mathrm{bin}}(\gamma)\right]^{H} \left[1 - P_{\mathrm{e}}(\gamma)\right]^{L_{\mathrm{P}}} \quad . \tag{60}$$

Above, $P_{\mathrm{e}}(\gamma)$ can be computed using

$$P_{\mathrm{e}}(\gamma) \approx \sum_{\kappa=d_{\mathrm{free}}}^{\infty} \beta_{\kappa} P_2(\kappa) \ , \tag{61}$$

where β_κ are the information weight of the codewords that are at a distance κ of the all zero codewords, d_{free} is the minimum distance of the code, and [43, pg. 491]

$$P_2(\kappa) = \begin{cases} \sum\limits_{j=\frac{\kappa+1}{2}}^{\kappa} \binom{\kappa}{j} \left[1 - P_{\mathrm{b}}(\gamma)\right]^{\kappa-j} P_{\mathrm{b}}(\gamma)^{j} & \text{if } \kappa \text{ is odd, and} \\ \frac{1}{2}\binom{\kappa}{\frac{\kappa}{2}} [1 - P_{\mathrm{b}}(\gamma)]^{\kappa/2} P_{\mathrm{b}}(\gamma)^{\kappa/2} & \\ \quad + \sum\limits_{j=\frac{\kappa}{2}+1}^{\kappa} \binom{\kappa}{j} [1 - P_{\mathrm{b}}(\gamma)]^{\kappa-j} P_{\mathrm{b}}(\gamma)^{j} & \text{if } \kappa \text{ is even.} \end{cases} \tag{62}$$

APPENDIX C
ANALYTICAL EXPRESSIONS IN TERMS OF THE FER

This section derives expressions for the mean number of transmission trials, $\bar{\tau}$, and the outage probability, q_z (c.f. Section II-A5) for S-HARQ in terms of the FER of the t-th transmission trial $P_{\mathrm{f}}(t)$.

In general, the event of needing $\tau = t \leq z$ transmission trials to get a correctly decoded frame is equivalent to have a correct transmission in the t-th trial and $t-1$ frames with errors in the previous attempts. Let us define $\boldsymbol{h} = (h_1, h_2, \dots)$ as the succession of random variables which correspond to successive narrowband baseband-equivalent channel coefficients. Also, let us denote as $\mathfrak{e}_t$ (resp. $\mathfrak{s}_t$) the event of making an error while decoding the frame (resp. having a successful transmission) during the t-th transmission attempt.

Each transmission trial is affected by both the realization of the channel and the thermal noise. Note that the events $\mathfrak{e}_1, \dots, \mathfrak{e}_{t-1}, \mathfrak{s}_t$ are conditionally independent given the channel realization, as successive realizations of the thermal noise are by definition independent of each other. Therefore, the conditional p.d.f. of the random variable τ for a given channel

realization $\boldsymbol{h}$ can be expressed as $\mathbb{P}\{\tau = 1|\boldsymbol{h}\} = 1 - P_{\rm f}(1)$ for $t = 1$, and

$$\mathbb{P}\{\tau = t|\boldsymbol{h}\} = \mathbb{P}\{\mathfrak{s}_t \cup \mathfrak{e}_{t-1} \cup \cdots \cup \mathfrak{e}_1|\boldsymbol{h}\} \tag{63}$$

$$= \mathbb{P}\{\mathfrak{s}_t|\boldsymbol{h}\} \prod_{u=1}^{t-1} \mathbb{P}\{\mathfrak{e}_u|\boldsymbol{h}\} \tag{64}$$

$$= [1 - P_{\rm f}(t)] \prod_{u=1}^{t-1} P_{\rm f}(u) \ , \tag{65}$$

for $t \geq 2$. In the case of S-HARQ, the $P_{\rm f}(t)$ are random variables that depend on the frame size, modulation type and received SNR during the t-th trial. In particular, the cases of fast-fading and block-fading scenarios are analyzed in the following.

Let us now calculate an expression for q_z, as defined in Section III-A. Using its definition and (65) one can find that

$$q_z = 1 - \mathbb{E}\left\{\mathbb{P}\{\tau \leq z|\boldsymbol{h}\}\right\} \tag{66}$$

$$= 1 - \mathbb{E}\left\{\sum_{t=1}^{x} \mathbb{P}\{\tau = t|\boldsymbol{h}\}\right\} \tag{67}$$

$$= \mathbb{E}\left\{P_{\rm f}(1) - \sum_{t=2}^{z}\left(\prod_{u=1}^{t-1} P_{\rm f}(u) - \prod_{u=1}^{t} P_{\rm f}(u)\right)\right\} \tag{68}$$

$$= \mathbb{E}\left\{\prod_{u=1}^{z} P_{\rm f}(u)\right\} \ . \tag{69}$$

Let us now calculate $\bar{\tau}_z$. Using its definition given in (22), it can be seen that $\bar{\tau}_z = 1$ for $z = 1$, and

$$\bar{\tau}_z = \frac{1}{1 - q_z} \sum_{t=1}^{z} t \cdot \mathbb{E}\left\{\mathbb{P}\{\tau = t|\boldsymbol{h}\}\right\} \tag{70}$$

$$= \frac{1}{1 - q_z} \mathbb{E}\left\{1 - P_{\rm f}(1) + \sum_{t=2}^{z} t\left(\prod_{u=1}^{t-1} P_{\rm f}(u) - \prod_{u=1}^{t} P_{\rm f}(u)\right)\right\} \tag{71}$$

$$= \frac{1}{1 - q_z} \mathbb{E}\left\{1 - z\prod_{u=1}^{z} P_{\rm f}(u) + \sum_{t=1}^{z-1}\prod_{u=1}^{t} P_{\rm f}(u)\right\} \tag{72}$$

when $z \geq 2$.

Finally, let us calculate $\bar{\tau}$. When $z = 1$ it is clear, using (23) and (69), that $\bar{\tau} = 1/(1 - \mathbb{E}\left\{P_{\rm f}\right\})$. For the case of $z \geq 2$, using (23), (69) and (72) one finds that

$$\bar{\tau} = z\frac{q_z}{1 - q_z} + \bar{\tau}_z \tag{73}$$

$$= \frac{\mathbb{E}\left\{1 + \sum_{t=1}^{z-1}\prod_{u=1}^{t} P_{\rm f}(u)\right\}}{1 - \mathbb{E}\left\{\prod_{u=1}^{z} P_{\rm f}(u)\right\}} \ . \tag{74}$$

APPENDIX D
MONOTONICITY OF (31)

Let us show that $\Delta(z) = \bar{\tau}^{\text{bf}}(z+1) - \bar{\tau}^{\text{bf}}(z) \geq 0$ for all $z \in \mathbb{N}$, with $\bar{\tau}^{\text{bf}}(z)$ as defined in Section II-A5. To do this, the following inequality is required (which is a direct application of Jensen's inequality):

$$\mathbb{E}\left\{P_{\text{f}}^{z}\right\} \geq \mathbb{E}\left\{P_{\text{f}}\right\}^{z} \quad , \tag{75}$$

which is valid for any positive integer z. Note that two successive applications of (75) give

$$\sum_{t=0}^{z-1} \mathbb{E}\left\{P_{\text{f}}^{t}\right\} \geq \sum_{t=0}^{z-1} \mathbb{E}\left\{P_{\text{f}}\right\}^{t} = \frac{1-\mathbb{E}\left\{P_{\text{f}}\right\}^{z}}{1-\mathbb{E}\left\{P_{\text{f}}\right\}} \geq \frac{1-\mathbb{E}\left\{P_{\text{f}}^{z}\right\}}{1-\mathbb{E}\left\{P_{\text{f}}\right\}} \quad . \tag{76}$$

Now, by considering (30), one can show the following:

$$\Delta(z) = \frac{\mathbb{E}\left\{P_{\text{f}}^{z}\right\}}{1-\mathbb{E}\left\{P_{\text{f}}^{z+1}\right\}} + \dots \tag{77}$$

$$\dots + \left(\frac{1}{1-\mathbb{E}\left\{P_{\text{f}}^{z+1}\right\}} - \frac{1}{1-\mathbb{E}\left\{P_{\text{f}}^{z}\right\}}\right) \sum_{t=0}^{z-1} \mathbb{E}\left\{P_{\text{f}}^{t}\right\} \tag{78}$$

$$\geq \frac{\mathbb{E}\left\{P_{\text{f}}^{z}\right\}}{1-\mathbb{E}\left\{P_{\text{f}}^{z+1}\right\}} + \frac{\mathbb{E}\left\{P_{\text{f}}^{z+1}\right\} - \mathbb{E}\left\{P_{\text{f}}^{z}\right\}}{(1-\mathbb{E}\left\{P_{\text{f}}^{z+1}\right\})(1-\mathbb{E}\left\{P_{\text{f}}\right\})} \tag{79}$$

$$= \frac{\mathbb{E}\left\{P_{\text{f}}^{z+1}\right\} - \mathbb{E}\left\{P_{\text{f}}\right\}\mathbb{E}\left\{P_{\text{f}}^{z}\right\}}{(1-\mathbb{E}\left\{P_{\text{f}}^{z+1}\right\})(1-\mathbb{E}\left\{P_{\text{f}}\right\})} \tag{80}$$

$$\geq \frac{\mathbb{E}\left\{P_{\text{f}}^{z+1}\right\} - \mathbb{E}\left\{P_{\text{f}}\right\}^{z+1}}{(1-\mathbb{E}\left\{P_{\text{f}}^{z+1}\right\})(1-\mathbb{E}\left\{P_{\text{f}}\right\})} \tag{81}$$

$$\geq 0 \ . \tag{82}$$

Above, (79) is a consequence of (76), while (81) and (82) are applications of (75).

ACKNOWLEDGMENT

This work was partially funded by CONICYT of Chile with projects 15110017 FONDAP 2011 and FONDEF IT13i20015.

REFERENCES

[1] A. W. Holger Karl, *Protocols and Architectures for Wireless Sensor Networks*. John Wiley & Sons inc., 2005.

[2] R. Verdone, D. Dardari, G. Mazzini, and A. Conti, *Wireless Sensor and Actuator Network: technologies, analysis and design*. Academic Press, 2008.

[3] K. Martinez, P. Padhy, A. Elsaify, G. Zou, A. Riddoch, J. K. Hart, and H. L. R. Ong, "Deploying a Sensor Network in an Extreme Environment." *Sensor Networks, Ubiquitous and Trustworthy Computing*, vol. 5-7, pp. 186–193, 2006.

[4] F. Rosas and C. Oberli, "Modulation and SNR optimization for achieving energy-efficient communications over short-range fading channels," *IEEE Transactions on Wireless Communications*, vol. 11, no. 12, pp. 4286–4295, 2012.

[5] ——, "Impact of transmitter-side CSI on the energy-efficiency of MIMO communications," *IEEE Trans. Wireless Commun.*, under revision.

[6] I. Stanojev, O. Simeone, Y. Bar-Ness, and D. H. Kim, "Energy efficiency of non-collaborative and collaborative hybrid-ARQ protocols," *IEEE Transactions on Wireless Communications*, vol. 8, no. 1, pp. 326–335, Jan 2009.

[7] Y. Li, G. Ozcan, M. Gursoy, and S. Velipasalar, "Energy efficiency of hybrid-ARQ systems under QoS constraints," in *48th Annual Conference on Information Sciences and Systems (CISS)*, March 2014, pp. 1–6.

[8] B. Makki, T. Svensson, T. Eriksson, and M.-S. Alouini, "Adaptive space-time coding using ARQ," *IEEE Transactions on Vehicular Technology*, vol. PP, no. 99, pp. 1–1, 2014.

[9] G. Li, Z. Xu, C. Xiong, C. Yang, S. Zhang, Y. Chen, and S. Xu, "Energy-efficient wireless communications: tutorial, survey, and open issues," *IEEE Wireless Communications*, vol. 18, no. 6, pp. 28 –35, Dec. 2011.

[10] C. Isheden, Z. Chong, E. Jorswieck, and G. Fettweis, "Framework for link-level energy efficiency optimization with informed transmitter," *IEEE Transactions on Wireless Communications*, vol. 11, no. 8, pp. 2946–2957, August 2012.

[11] S. L. Howard, C. Schlegel, and K. Iniewski, "Error control coding in low-power wireless sensor networks: When is ECC energy-efficient?" *EURASIP Journal on Wireless Communications and Networking*, no. 2006, p. 14, 2006.

[12] J. H. Kleinschmidt, W. C. Borelli, and M. E. Pellenz, "An energy efficiency model for adaptive and custom error control schemes in bluetooth sensor networks," *AEU - International Journal of Electronics and Communications*, vol. 63, no. 3, pp. 188–99, 2009.

[13] J. H. Kleinschmidt, "Analyzing and improving the energy efficiency of IEEE 802.15.4 wireless sensor networks using retransmissions and custom coding," *Telecommunication Systems*, pp. 1–7, 2013.

[14] M. E. Pellenz, R. D. Souza, and M. S. P. Fonseca, "Error control coding in wireless sensor networks," *Telecommunication Systems*, vol. 44, no. 1-2, pp. 61–68, 2010.

[15] F. Vacirca, A. De Vebductis, and A. Baiocchi, "Optimal design of hybrid FEC/ARQ schemes for TCP over wireless links with Rayleigh fading," *IEEE Transactions on Mobile Computing*, vol. 5, no. 4, pp. 289–302, Apr. 2006.

[16] Y. Sankarasubramaniam, I. Akyildiz, and S. McLaughlin, "Energy efficiency based packet size optimization in wireless sensor networks," in *Proceedings of the First IEEE International Workshop on Sensor Network Protocols and Applications*, 2003, pp. 1–8.

[17] J. Wu, G. Wang, and Y. Zheng, "Energy and spectral efficient transmissions of coded ARQ systems," in *IEEE International Conference on Communications (ICC)*, June 2013, pp. 5883–5887.

[18] ——, "Energy efficiency and spectral efficiency tradeoff in type-I ARQ systems," *IEEE Journal on Selected Areas in Communications*, vol. 32, no. 2, pp. 356–366, February 2014.

[19] F. Rosas, G. Brante, R. Souza, and C. Oberli, "Optimizing the code rate for achieving energy-efficient wireless communications," in *Proc. WCNC'14*, April 2014, pp. 787–792.

[20] T. H. Lee, *The Design of CMOS Radio-Frequency Integrated Circuits*. Cambridge University Press, 1998.

[21] S. Cui, A. J. Goldsmith, and A. Bahai, "Energy-constrained modulation optimization," *IEEE Transactions on Wireless Communications*, vol. 4, no. 5, pp. 2349–2360, 2005.

[22] T. S. Rappaport, *Wireless Communications: Principles and Practice*. Upper Saddle River, NJ, USA: Prentice Hall, 2002.

[23] A. Sinha and A. Chandrakasan, "Dynamic power management in wireless sensor networks," *IEEE Design & Test of Computers*, vol. 18, no. 2, pp. 62–74, 2001.

[24] S. Lin, J. Costello, D.J., and M. Miller, "Automatic-repeat-request error-control schemes," *IEEE Communications Magazine*, vol. 22, no. 12, pp. 5–17, December 1984.

[25] A. Goldsmith, *Wireless Communications*. Cambridge University Press, 2005.

[26] M. Loeve, *Probability Theory I*. Springer, 1978.

[27] D. Chase, "Code Combining–A Maximum-Likelihood Decoding Approach for Combining an Arbitrary Number of Noisy Packets," *IEEE Transactions on Communications*, vol. 33, no. 5, pp. 385–393, May 1985.

[28] M. Nakagami, "The m-distribution, a general formula of intensity of rapid fading," in *Statistical Methods in Radio Wave Propagation: Proceedings of a Symposium held June 18-20, 1958*, W. C. Hoffman, Ed. Pergamon Press., 1960, pp. pp. 3–36.

[29] F. Rosas and C. Oberli, "Nakagami-m approximations for multiple-input multiple-output singular value decomposition," *IET Transactions on Communications*, vol. 7, no. 6, pp. 554–561, April 2013.

[30] S. Boyd and L. Vandenberghe, *Convex Optimization*. New York, NY, USA: Cambridge University Press, 2004.

[31] *European Standard (Telecomunication Series)*, ETSI Std. EN 300 440-1 v1.5.1, 2010.

[32] I. Bocharova and B. Kudryashov, "Rational rate punctured convolutional codes for soft-decision viterbi decoding," *IEEE Transactions on Information Theory*, vol. 43, no. 4, pp. 1305–1313, 1997.

[33] G. Begin, D. Haccoun, and C. Paquin, "Further results on high-rate punctured convolutional codes for viterbi and sequential decoding," *IEEE Transactions on Communications*, vol. 38, no. 11, pp. 1922–1928, 1990.

[34] *Specifications for Local and Metropolitan Area Networks- Specific Requirements Part 15.4: Wireless Medium Access Control (MAC) and Physical Layer (PHY)*, IEEE Std. 802.15.4-2006, 2006.

[35] A. Bannoura, O. Gorgis, L. Reindl, and C. Schindelhauer, "Time analysis for wireless wake-up radio transceivers," in *Proceedings SENSOR 2013 AMA conferences*, 2013.

[36] T. Instruments, "MSP430BT5190 Product Review," Online, 2010.

[37] A. He, S. Srikanteswara, K. K. Bae, T. Newman, J. Reed, W. Tranter, M. Sajadieh, and M. Verhelst, "System power consumption minimization for multichannel communications using cognitive radio," in *IEEE COMCAS*, Nov 2009, pp. 1–5.

[38] L. Zhang et al., "A Reconfigurable Sliding-IF Transceiver for 400 MHz/2.4 GHz IEEE 802.15.6/ZigBee WBAN Hubs With Only 21% Tuning Range VCO," *IEEE Journal of Solid-State Circuits*, vol. 48, no. 11, pp. 2705–2716, Nov 2013.

[39] F. Rosas, R. D. Souza, and C. Oberli, "Comparative analysis of the optimization of error correcting codes and MIMO SVD schemes for increasing the energy efficiency of communications," in *Proceedings of the 4th joint WIC/IEEE SP Symposium on Information Theory and Signal Processing in the Benelux*, May 2014.

[40] S. Lin and D. J. Costello, *Error Control Coding: Fundamentals and Applications*, 2nd ed. Prentice-Hall, June 2004.

[41] R. McEliece and W. Lin, "The trellis complexity of convolutional codes," *Information Theory, IEEE Transactions on*, vol. 42, no. 6, pp. 1855–1864, 1996.

[42] I. B. Benchimol, C. Pimentel, R. Demo Souza, and B. F. Uchoa-Filho, "A computational complexity measure for trellis modules of convolutional codes," in *36th International Conference on Telecommunications and Signal Processing (TSP)*, 2013, pp. 144–148.

[43] J. Proakis, *Digital Communications*. McGraw-Hill, 2001.